Phason-disordered two-dimensional quantum antiferromagnets

Attila Szallas
CNR-INFM-National Research Center on Nano-Structures and Bio-Systems at Surfaces (S3), Via Campi 213/A, 41100 Modena, Italy

Anuradha Jagannathan
Laboratoire de Physique des Solides, CNRS-UMR 8502, Université Paris-Sud, 91405 Orsay, France

Stefan Wessel
Institut für Theoretische Physik, Universität Stuttgart, 70550 Stuttgart, Germany
(Received 27 January 2009; published 14 May 2009)

We examine a type of disorder that is unusual in the context of quantum antiferromagnets although well known in the literature of quasiperiodic systems. Our model consists of localized spins with antiferromagnetic exchanges on a bipartite quasiperiodic structure, which is geometrically disordered in such a way that no frustration is introduced. In the limit of zero disorder, the structure is the perfect Penrose rhombus tiling. This tiling is progressively disordered by augmenting the number of random "phason flips" or local tile-reshuffling operations. The ground state remains Néel ordered, and we have studied its properties as a function of increasing disorder using linear spin-wave theory and quantum Monte Carlo. We find that the ground-state energy decreases, indicating *enhanced* quantum fluctuations with increasing disorder. The magnon spectrum is progressively smoothed, and the effective spin-wave velocity of low-energy magnons increases with disorder. For large disorder, the ground-state energy as well as the average staggered magnetization tend toward limiting values characteristic of this type of randomized tilings.

DOI: 10.1103/PhysRevB.79.172406 PACS number(s): 75.10.Jm, 71.23.Ft

This Brief Report discusses the effects of a type of disorder called phason disorder on the ground state of Heisenberg antiferromagnets. The clean system is a perfectly deterministic quasiperiodic two-dimensional (2D) tiling, and the type of disorder we consider is geometrical, involving a discrete shift of a randomly selected subset of sites. These phason flips are operations that correspond to reorganizing the structure locally in the vicinity of the flipped site. This type of disorder is strongly constrained, as one does not modify the basic building blocks of the structure, but only the way they are connected. For many quasicrystalline alloys, samples of good quality are believed to possess long-range order with some thermally induced phonon and phason disorder present at finite temperatures.[1] However, one can also consider essentially random quasiperiodic structures, which could be preferred for entropic reasons.[2]

Quenched phason disorder has been considered previously in other contexts, in particular, concerning electronic properties, and the possibility of Anderson localization in such systems was discussed. Benza *et al.*[3] considered quantum diffusion in a two-dimensional randomized tiling and found that the typical value of the diffusion exponent was larger for the disordered system compared to the pure case. This means that quasicrystals show delocalizationlike effects from disorder rather than the opposite, weak localization due to disorder, observed in periodic systems. Piechon and Jagannathan[4] came to the same conclusion by analyzing the statistics of the energy levels in phason-disordered tilings (see, e.g., Refs. 5 and 6 for reviews). Schwabe *et al.*[7] analyzed the effect of phason flips on the electronic levels and wave functions, showing that they lead to a smoothing of the density of states, as well as of the fluctuations of the conductance. Finally, the effects of randomness on the phonon spectrum has been considered in two-dimensional quasiperiodic tilings (see, e.g., Ref. 8).

The study of the Heisenberg model on a quasiperiodic tiling is motivated by experimental findings of antiferromagnetic correlations in quasiperiodic ZnMgR alloys (R: rare earth).[9] In theoretical models considered thus far[10–14] bipartite tilings are considered, with all sites occupied by spins, and their exchanges restricted to adjacent lattice sites, such that no frustration arises. Furthermore, these studies did not take into account the effects of disorder, which is almost certainly also present in the experimentally studied alloys. Here, we focus on the effects that arise in quasiperiodic magnets in the presence of phason disorder, which is found to lead to enhanced quantum fluctuations, as indicated by the lowering of the ground-state energy along with a reduction in the staggered magnetization with increasing disorder.

Figure 1 shows a portion of a perfect (deterministic) Penrose tiling and a typical example of a phason-disordered tiling. We consider in the following the antiferromagnetic spin-$\frac{1}{2}$ Heisenberg model with Hamiltonian $H=J\Sigma_{\langle i,j\rangle}\mathbf{S}_i\cdot\mathbf{S}_j$ for spins $\mathbf{S}_i$ located on all vertices of such tilings. Nearest-neighbor exchanges are antiferromagnetic $J>0$ and act between pairs of sites that are linked by an edge. Despite the fact that all couplings are equal, the ground state is spatially inhomogeneous contrary to, e.g., the square lattice antiferromagnet, where the staggered magnetization is uniform. The local staggered magnetizations vary as a function of the local environment, and the ground state takes a complex hierarchically organized structure.[10–14] The disorder considered here is purely geometric; i.e., the coupling J along bonds remains fixed at a constant value.

Using linear spin-wave theory (LSWT) and quantum Monte Carlo (QMC) calculations, we consider periodic approximants of the Penrose tiling.[13,14] These are finite samples

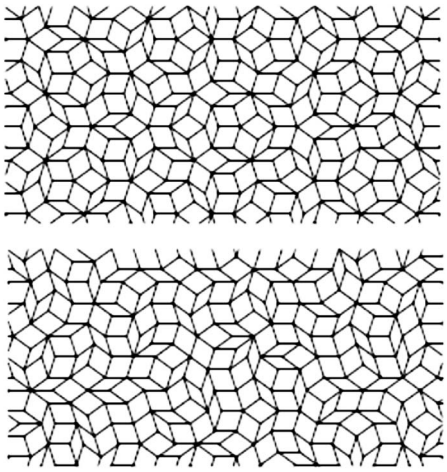

FIG. 1. Illustration of a perfect (upper panel) and a phason-disordered Penrose tiling (lower panel).

of N spins, satisfying periodic boundary conditions. Perfect tilings are obtained by the cut-and-project method (see, e.g., Ref. 14) after which they are disordered by the following method: A phason flip is a process by which a threefold site hops to a new allowed position (in terms of the tile configurations). The old site disappears, as do the three bonds linking it to its neighbors, while a new threefold site appears on the other sublattice (Fig. 2). In our phason generating procedure, we randomly select a threefold site. If $\vec{r}_0$ and $\vec{r}_i$ $(i=1,2,3)$ denote the position vectors of the central site and its three neighbors, the new position of the site is given by $\vec{r}_0'-\vec{r}_0=\Sigma_{j=1}^{3}(\vec{r}_j-\vec{r}_0)$ (Fig. 2). Three new bonds appear linking the new site to the sites at the positions $\vec{r}_j'$ $(j=1,2,3)$. The coordination numbers of all of the seven sites involved are updated, and the whole procedure is repeated, with the constraint that there be an equal number of flipped sites on the A and the B sublattices, so as to preserve the condition $N_A=N_B$, where N_A (N_B) denotes the number of sites of the A (B) sublattice.

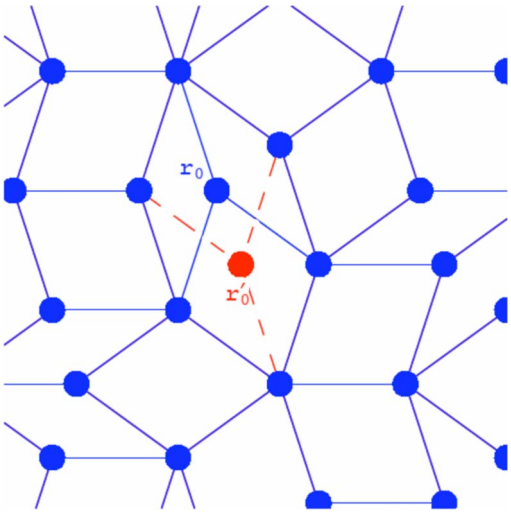

FIG. 2. (Color online) A single phason flip, showing the original (r_0) and final (r_0') positions of the shifted lattice site. New edges are shown by dashed lines.

For a given total number of phason flips N_{ph}, the degree of disorder Δ is defined as the average overlap distance between the perfect sample and the disordered samples. The overlap for a given sample is defined by $N^{-1}\Sigma_{i=1}^{N}\eta_i$, where η_i is 1 or 0, depending on whether site i is shifted or not with respect to the perfect tiling. The whole procedure is then repeated for approximants of system sizes $N=246$, 644, 1686, and 4414 in LSWT and 246, 644, and 1686 in QMC. Averaging is carried out over a large number of samples: 100 samples for $N=246$, 644, and 1686 and 10 samples for $N=4414$ in LSWT, and 40 samples for $N=246$ and 20 samples for $N=644$ and 1686 in the QMC. This method of disordering does not change the overall number of rhombi of each kind and generates samples of fixed phason strain.[15] Due to the fact that we start out with a defected structure (a periodic approximant, which is only locally equivalent to the infinite quasiperiodic tiling) there is an upper limit to the number of phason flips we are able to introduce in the tilings. Unacceptable configurations are observed to appear after a number of flips larger than about $1.3N$, corresponding to the number of steps after which the periodic boundary conditions are felt by the system.

After the randomized samples are obtained, LSWT calculations are performed as described in Refs. 12 and 14. Spin operators are transformed using the Holstein-Primakoff transformation to bosonic operators a_i and b_j $(i,j=1,\ldots,N/2)$, corresponding to the A and B sublattices, respectively. The linearized Hamiltonian in the boson operators is then diagonalized numerically. Once the eigenmodes have been determined, one obtains the ground-state energy, and local staggered magnetizations for each realization of disorder. Finally, we carry out the statistical analysis of the results by performing disorder averaging. Within the QMC simulations, we obtain the local staggered magnetization $m_s^2(i)=\frac{3}{N}\Sigma_{j=1}^{N}\epsilon_i\epsilon_j\langle S_i^z S_j^z\rangle$ from the spin-spin correlation function,[10,12] where $\epsilon_i=\pm 1$, depending on whether lattice site i belongs to sublattice A or B. The QMC simulations were performed using the stochastic series expansion method[16] at temperatures taken low enough to obtain ground-state properties of these finite systems.[12]

We now describe our results on the effect of phason disorder. First, we consider the average ground-state energy per site E_0/N, shown as a function of disorder in Fig. 3 for the $N=4414$ sites system. The values have been normalized with respect to the value obtained for the clean system. Also shown is a fit to an exponential decay toward a limiting value in the strong disorder case, of the form $E_0/N=e_{\mathrm{dis}}+(e_{\mathrm{perf}}-e_{\mathrm{dis}})e^{-a\Delta}$, with $a=11.16$, $e_{\mathrm{dis}}=-0.6500$, and $e_{\mathrm{perf}}=-0.6429$. The asymptotic value of the ground-state energy e_{dis} represents the average value of the ground-state energy of maximally randomized Penrose approximants, which lies below the ground-state energy of the perfect system. This indicates that the introduction of phasons tends to enhance quantum fluctuations in the tilings, as compared to the clean case. The inset of Fig. 3 shows the ground-state energy per site as a function of disorder, obtained from LSWT and QMC simulations, normalized with respect to the value obtained for the clean system. The results obtained from LSWT and QMC are found to be in good agreement. This also shows the applicability of the linear spin-wave approximations to this randomized system.

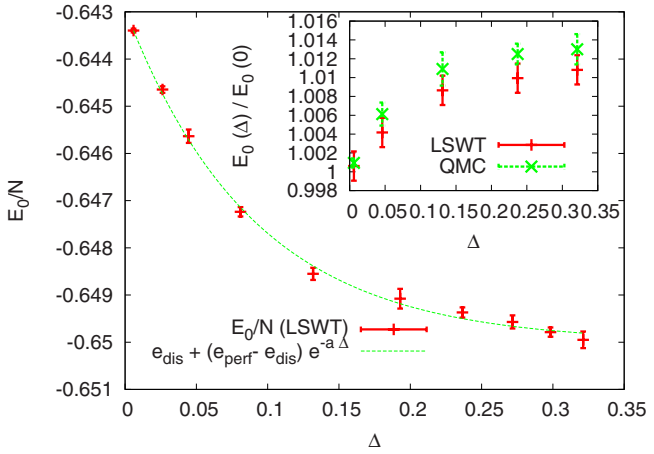

FIG. 3. (Color online) Dependence of the ground-state energy on the disorder strength Δ calculated within LSWT. The smooth curve is a fit to an exponential decay toward a higher disorder value. The system size $N=4414$. The inset shows the normalized ground-state energy as a function of disorder Δ. Points represent values obtained after scaling LSWT and QMC data to infinite system sizes.

Next, we consider the density of states defined by $\rho(E) = \frac{1}{N}\Sigma_{m=1}^{N}\delta(E-\omega_m)$, where ω_m are the eigenvalues found by numerical diagonalization. Figure 4 shows the density of states, $\rho(E)$ (smoothed by replacing the delta function by a Gaussian of fixed small width, so as to eliminate the most rapid fluctuations), plotted as a function of E for several values of the disorder strength. The figure shows that main effects of phason disorder on the density of states is to progressively flatten and broaden the peaks, leading to a smoothening of fluctuations and filling in of gaps. Similar behavior is seen in the electronic case.[5] The low-energy tail is linear and can be fitted to obtain the averaged low-energy spin-wave velocity $\bar{c}$, which *increases* with Δ as shown in the inset of Fig. 5. This indicates that spin-wave propagation is facilitated by the phason disorder, in analogy with the problem of quantum diffusion of electrons in the tight-binding model in quasiperiodic tilings.[5] In addition, the localized states at $E=3$ disappear progressively. These states

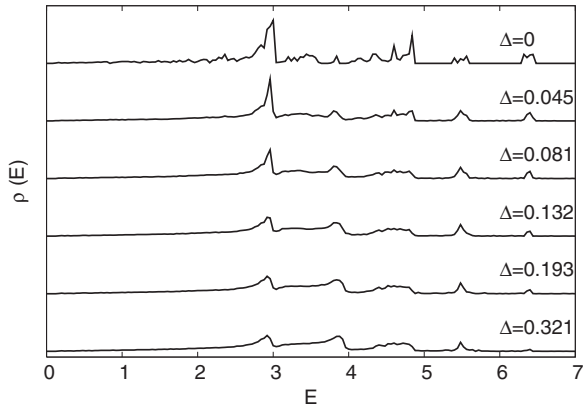

FIG. 4. Evolution of the density of states $N(E)$ for various values of the disorder strength Δ from LSWT on the $N=4414$ sites system.

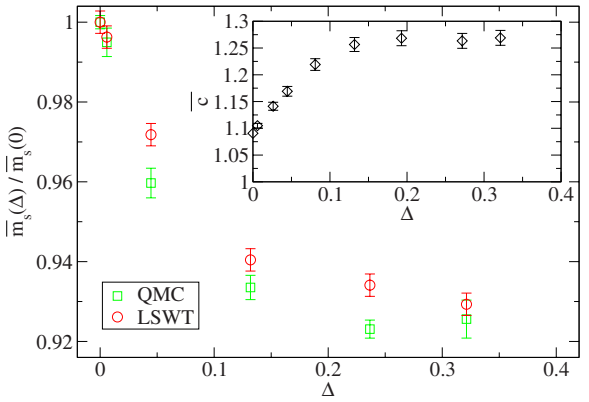

FIG. 5. (Color online) Normalized averaged staggered magnetization as a function of phason disorder strength Δ. Points represent values obtained from LSWT and QMC data after scaling to the thermodynamic limit. The inset shows the averaged spin-wave velocity $\bar{c}$ as a function of the disorder strength Δ as obtained within LSWT.

arise on closed loops of threefold sites.[14] They are hence destroyed when a phason flip occurs on one of the participating sites.

Finally, we turn to discuss the evolution of the staggered magnetization upon introducing phason disorder. Figure 5 shows the spatial average of the staggered magnetization (i.e., after averaging over all of the sites) as a function of disorder, normalized with respect to the value obtained for the clean system. The curve shows a clear decrease in the global staggered magnetization with increasing disorder. As for the ground-state energy curve, the decrease eventually levels off. It is also interesting to analyze the evolution of the full distribution of the staggered magnetizations with increasing phason disorder. In the perfect tiling, this distribution has several peaks, each of which corresponds to a distinct coordination number. In the disordered tilings, the differences between the coordination numbers are smoothed out. As Fig. 6 shows, the distribution becomes smoother, as the disorder is increased. In addition, the average value shifts to lower values. The smoothing occurs due to a larger number of local environments created by the phason flips and due

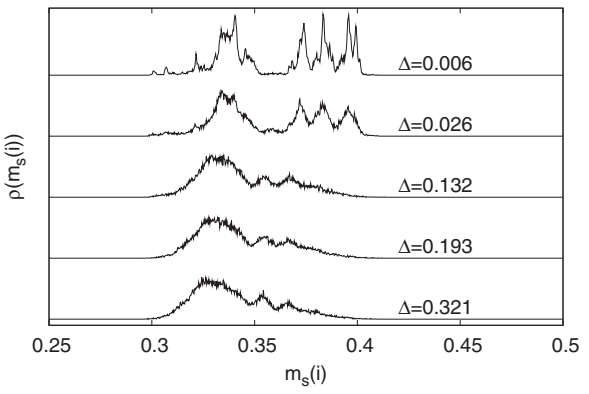

FIG. 6. Evolution of the distribution in the local staggered magnetization with the disorder strength, as obtained within LSWT on the 4414 sites system.

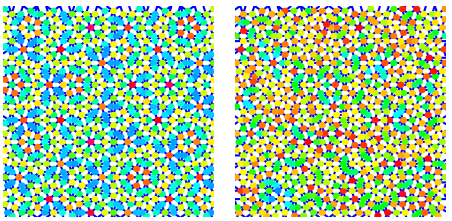

FIG. 7. (Color online) Color representation of the local staggered magnetizations in a perfect tiling (left) and a disordered tiling (right) showing sites of magnetizations ranging from high (blue online) to low (red online) values.

to the loss of self-similarity on larger length scales.

Figure 7 is a representation of the magnetization values in a small portion of the tiling for the perfect and the disordered cases. The distribution is more homogeneous in the disordered tiling, which furthermore lacks the hierarchical features of the perfect tiling. In the color plot, one can also note that the disordered ground state (right hand figure) possesses a reddish tone compared to the perfect ground state (left hand figure), illustrating the already noted fact that globally the staggered magnetization is lower in the disordered system.

In conclusion, we analyzed the effects of geometrical disorder on the magnetic properties of quasiperiodic antiferromagnets. Concerning the low-energy modes, magnons propagate with a slightly higher velocity in the disordered tiling as compared to the perfect quasiperiodic tiling. The density of states is smoothed. Degenerate states localized on closed loops disappear with increasing disorder. Eigenmodes tend to become more delocalized as compared to the perfect tiling. These effects have their analogy in phonon models, as well as in the tight-binding model for electrons in quasiperiodic tilings. In the magnetic problem our results also indicate that the effect of disorder is to reduce the strong coherent backscattering of the magnon wave functions due to a perfect quasiperiodic potential and to favor a more diffusive dynamics. Upon increasing phason disorder in the antiferromagnetic model, the ground state progressively loses its self-similar features and tends toward a more homogeneous distribution of staggered moments. The global average of the staggered magnetization decreases, as does the ground-state energy, signaling increased quantum spin fluctuations. Both quantities tend toward a limiting value for this class of disordered tilings. Such two-dimensional quantum antiferromagnets may be experimentally realizable in the near future, as there has been considerable progress recently with depositing atoms on quasiperiodic surfaces, which serve as templates. A monolayer of Pb atoms having quasiperiodic symmetry has been obtained.[17] To study quantum magnetism one needs to obtain such a surface layer using low-spin atoms. In addition, one needs the interactions to be predominantly short range and antiferromagnetic, and this could be realized via a superexchange mechanism, as in the cuprate layers of high T_c compounds, in which oxygen atoms mediate the exchange between the $S=\frac{1}{2}$ copper spins.

We thank HLRS Stuttgart and NIC Jülich for allocation of computing time. A.S. was supported by the European Commission, through a Marie Curie Foundation under Contract No. MEST CT 2004-51-4307, during the course of this work.

[1] P. J. Steinhardt and S. Ostlund, *The Physics of Quasicrystals* (World Scientific, Singapore, 1987).
[2] C. L. Henley, Philos. Mag. **86**, 1123 (2005).
[3] B. Passaro, C. Sire, and V. G. Benza, Phys. Rev. B **46**, 13751 (1992).
[4] F. Piechon and A. Jagannathan, Phys. Rev. B **51**, 179 (1995)
[5] C. Sire, in *Lectures on Quasicrystals*, edited by F. Hippert and D. Gratias (Les Editions de Physique, Les Ulis, 1994).
[6] A. Jagannathan and F. Piechon, Philos. Mag. **87**, 2389 (2007).
[7] H. Schwabe, G. Kasner, and H. Böttger, Phys. Rev. B **59**, 861 (1999).
[8] J. Los, T. Janssen, and F. Gähler, Int. J. Mod. Phys. B **7**, 1505 (1993).
[9] T. J. Sato, H. Takakura, A. P. Tsai, K. Shibata, K. Ohoyama, and K. H. Andersen, Phys. Rev. B **61**, 476 (2000); T. J. Sato, H. Takakura, A. P. Tsai, and K. Shibata, *ibid.* **73**, 054417 (2006)
[10] S. Wessel, A. Jagannathan, and S. Haas, Phys. Rev. Lett. **90**, 177205 (2003).
[11] A. Jagannathan, Phys. Rev. B **71**, 115101 (2005).
[12] S. Wessel and I. Milat, Phys. Rev. B **71**, 104427 (2005).
[13] A. Jagannathan, A. Szallas, S. Wessel, and M. Duneau, Phys. Rev. B **75**, 212407 (2007).
[14] A. Szallas and A. Jagannathan, Phys. Rev. B **77**, 104427 (2008).
[15] In the cut-and-project scheme (see, e.g. Ref. 14) the deviations from perfect order correspond to fluctuations in which the orientation of the cut in five-dimensional space remains constant.
[16] A. W. Sandvik, Phys. Rev. B **59**, R14157 (1999).
[17] J. Ledieu, L. Leung, L. H. Wearing, R. McGrath, T. A. Lograsso, D. Wu, and V. Fournee, Phys. Rev. B **77**, 073409 (2008).